Available online at www.sciencedirect.com

ScienceDirect

IFAC Papers Online CONFERENCE PAPER ARCHIVE

IFAC-PapersOnLine 49-7 (2016) 448–453

Dynamic dimension reduction for thin-film deposition reaction network models

Raymond A. Adomaitis *

* *Chemical & Biomolecular Engineering, Institute for Systems Research, University of Maryland, College Park, MD 20742 USA (e-mail: adomaiti@umd.edu).*

Abstract: A prototype thin-film deposition model is developed and subsequently used in a sequence of model reduction procedures, ultimately reducing the dynamic dimension from six to one with essentially no loss in accuracy to the dynamics of the deposition process. The species balance model consists of a singular perturbation problem of nonstandard form which first is numerically solved following the approach of Daoutidis (2015). An alternative strategy then is presented, consisting of a reaction factorization procedure which facilitates the solution of the outer solution of the singular perturbation problem and provides unique physical insight into the conserved quantities (reaction invariants) identified by the elimination of redundant dynamic modes. Further reduction in dynamic dimension then is achieved through a second factorization focused only on the major reaction species. This second reduction procedure identifies pseudo-equilibria of finite-rate properties and introduces an additional level of complexity to the challenges of identifying consistent initial conditions for DAE systems.

Keywords: Differential equations; model reduction; singular perturbation method; time constants; chemical industry; reaction invariants

1. INTRODUCTION

There is a rich history of research in model reduction methods for chemical reaction networks, especially for homogenous systems. Recently, Daoutidis (2015) reviewed some of the reaction network model reduction literature in the context of differential-algebraic equations (DAEs) produced by the reduction procedure. The objective of this work is to present the details of implementing a reaction-factorization approach we have developed to reduce the dynamic dimension of thin-film deposition kinetics models; we compare it to methods presented in Daoutidis (2015) using a prototype deposition reaction model. Our motivation for dynamic model reduction is not for computational efficiency, but to understand the true minimal dynamic dimension of thin-film deposition models so as to obtain a better fundamental understanding of the dynamics of these processes.

Consider the simplified gas/surface reaction network (RN) and the net-forward rates associated with each reaction step listed in Table 1 and shown in Fig. 1 where M and D are gas-phase monomer and dimer species with number concentrations $[M]$ and $[D]$ in m^{-3}. Species A is an adsorbed surface species with number concentration $[A]$ m^{-2} while B represents the element of precursor M that is incorporated into the bulk film and $\mathrm{A}^{\ddagger}$ the transition state of the final irreversible reaction. Note that any by-products of the irreversible deposition reaction are omitted from this example. Sites open to adsorption S are consumed during adsorption of M and regenerated as bulk film B is created. The concentration of B $[B]$ also has units m^{-2}; its value can grow infinitely large because $[B]$ represents the total number of atoms deposited per unit surface area.

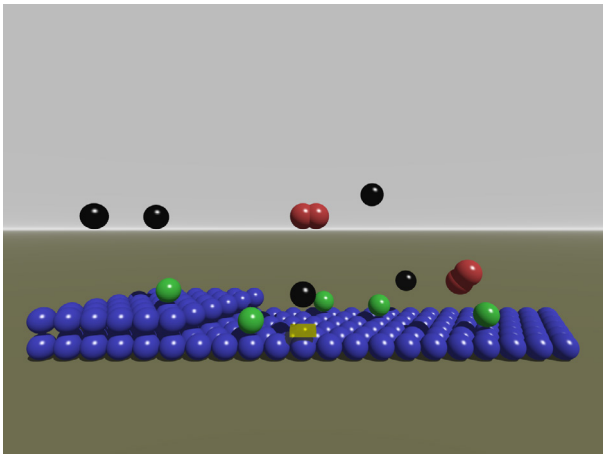

Fig. 1. A prototypical deposition system and the associated gas-phase and surface reactions. Monomer species M are shown in black, the dimer D in red, adatoms A in green, bulk film elements B in blue, and a representative adsorption site S as the yellow rectangular prism.

The first three reactions of Table 1 are reversible and the first is modeled as being barrierless in the forward direction, and so no transition state is defined for the adsorption process. The reaction between M and D is a gas phase reaction while the remainder are surface reactions.

⋆ The author gratefully acknowledges the support of the US National Science Foundation through grants CBET1160132 and CBET1438375.

10.1016/j.ifacol.2016.07.383

For this and other heterogeneous deposition RN, we can write the number concentration material balance for each species X_j, $j = 0, \ldots, n_s - 1$ as

$$\frac{d}{dt}\phi_i[X_j] = \frac{1}{\epsilon}\sum_{k=0}^{n_g-1} Q_{j,k}g_k + \sum_{k=0}^{n_f-1} P_{j,k}f_k \tag{1}$$

for phase ϕ_i, $i = 1, \ldots, n_p - 1$ where in our two-phase system ϕ_1 represents the area of the reaction surface (in m^2) and ϕ_0 the volume (m^3) of the gas phase. Of course (1) can be rewritten in terms of the vector of molar quantities $\mathbf{m}$ for the complete set species over all of the phases

$$\frac{d\mathbf{m}}{dt} = \frac{1}{\epsilon}\mathbf{Q}\mathbf{g} + \mathbf{P}\mathbf{f} \tag{2}$$

subject to the specified initial condition

$$\mathbf{m}(0) = \mathbf{m}_o \tag{3}$$

with species molar quantities and concentrations

$$\mathbf{m} = \begin{bmatrix} D \\ A \\ M \\ A^\ddagger \\ S \\ B \end{bmatrix} \qquad \mathbf{c} = \begin{bmatrix} [D] \\ [A] \\ [M] \\ [A^\ddagger] \\ [S] \\ [B] \end{bmatrix} = \begin{bmatrix} D/\phi_0 \\ A/\phi_1 \\ M/\phi_0 \\ A^\ddagger/\phi_1 \\ S/\phi_1 \\ B/\phi_1 \end{bmatrix}. \tag{4}$$

Reaction stoichiometic coefficients are split between the two arrays

$$\mathbf{Q} = \begin{bmatrix} 1 & 0 \\ 0 & -1 \\ -2 & 0 \\ 0 & 1 \\ 0 & 0 \\ 0 & 0 \end{bmatrix}, \quad \mathbf{P} = \begin{bmatrix} 0 & 0 \\ 1 & 0 \\ -1 & 0 \\ 0 & -1 \\ -1 & 1 \\ 0 & 1 \end{bmatrix},$$

with those net forward reactions that ultimately will be treated as equilibrium relations

$$\mathbf{g} = \begin{bmatrix} g_0 \\ g_1 \end{bmatrix} = \begin{bmatrix} \phi_0(K_0[M]^2 - [D]) \\ \phi_1(K_2[A] - [A^\ddagger]) \end{bmatrix} \tag{5}$$

and the finite-rate processes

$$\mathbf{f} = \begin{bmatrix} f_0 \\ f_1 \end{bmatrix} = \begin{bmatrix} \phi_1 k_1(K_1[M][S] - [A]) \\ \phi_1 k_3[A^\ddagger] \end{bmatrix}. \tag{6}$$

The time constant ϵ has units of (s) and should be thought of as an artificial construct that makes possible writing the species balance equations (2). Finite, but small, values of ϵ correspond to the reactions (5) dynamically relaxing to chemical equilibrium defined by $\mathbf{Q}\mathbf{g} = \mathbf{0}$. It is possible to solve (2-3) directly for finite ϵ using a numerical integration technique suitable for stiff problems, although this solution can only be considered the true solution when $\epsilon \to 0$.

To give some idea of the dynamics to be expected for the case $\epsilon \to 0$, let us first consider a numerical solution to (2) for small, but finite $0 < \epsilon \ll 1$. We first set $K_0 = K_1 = 1$ m^3, $K_2 = 1$, $k_1 = k_3 = 1$ s^{-1}, $\phi_1 = 1$ m^2, $\phi_0 = 1$ m^3 (these correspond to the values used in Adomaitis (2016) except for k_2 where it was set to a value of 2 in the cited work) and choose the specified initial condition (3) to be

$$\mathbf{m}_o = [0, 0, 1, 0, 1, 0]^\intercal. \tag{7}$$

noting that $\mathbf{m}_o$ and $\mathbf{c}_o$ will have numerically identical values given our selected values of ϕ_i.

Table 1. Elementary reaction steps and net-forward reaction rates.

reaction			net forward rate	
2M	$\leftrightharpoons$	D	$(1/\epsilon)g_0$	s^{-1} m^{-3}
S + M	$\leftrightharpoons$	A	f_0	s^{-1} m^{-2}
A	$\leftrightharpoons$	$A^\ddagger$	$(1/\epsilon)g_1$	s^{-1} m^{-2}
$A^\ddagger$	$\to$	B + S	f_1	s^{-1} m^{-2}

Recalling the elements of $\mathbf{m}$ in (4), the specified set of initial conditions of (7) corresponds to a pure monomer gas phase and a bare growth surface. Setting $\epsilon = 0.1$ s, we observe the dynamics of the 6 ODE system in Fig. 2 (left). In the time period shortly after $t = 0$, monomer M and dimer species D relax to a pseudo-equilibrium; that brief time segment is followed by a much longer period of consumption of M (and consequently D) through the adsorption process. Likewise, at a time scale that is slower than that of the gas-phase equilibration, we observe the saturation of the growth surface with A, a period that is also followed by a slow decay to zero. These dynamics are naturally mirrored by the those of the surface sites S. Finally, the bulk species B concentration continuously increases and only asymptotically ends as all gas- and surface-phase species are consumed. Overall, we observe three distinct time scales in the dynamics displayed in Fig. 2 (left).

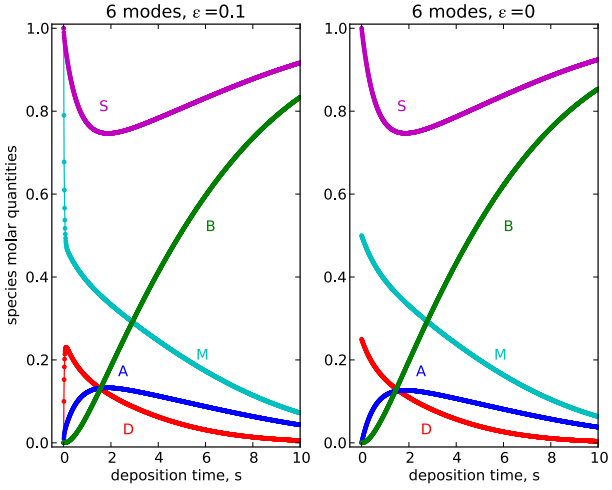

Fig. 2. Integration results for the six dynamic mode system for small finite ϵ (left) and $\epsilon \to 0$ (right).

2. SOLVING THE SINGULAR PERTURBATION PROBLEM

From Daoutidis (2015), we recognize (2) as a singularly perturbed system in nonstandard form. Because $\mathbf{Q}$ and $\partial\mathbf{g}/\partial\mathbf{m}$ are full column- and row-rank, respectively (this should be obvious by direct inspection), taking the limit $\epsilon \to 0$ will ultimately produce the pseudo-equilibrium manifold

$$\mathcal{Q} = \{\mathbf{m} : \mathbf{g} = \mathbf{0}, \mathbf{h} = \mathbf{0}\} \tag{8}$$

where the 4 additional relationships $\mathbf{h} = \mathbf{0}$ define the values of variables in $\mathbf{m}$ that are not computed using $\mathbf{g} = \mathbf{0}$. Defining the column vector γ by the elements

$$\gamma_i = \lim_{\epsilon \to 0} \frac{g_i}{\epsilon}$$